Molecular Genetics & Genomic Medicine

WILEY

Molecular Genetics & Genomic Medicine
Open Access

CLINICAL REPORT OPEN ACCESS

Genetic Insights Into Craniosynostosis: Identification of Novel *IL11RA* Variants in Chinese Pediatric Patients

Ziwei Liu[1] | Ding Zhou[2] | Chunli Wang[1] | Bixia Zheng[2] | Qing Yan[1] | Wei Zhou[2] | Gang Wang[1]

[1]Department of Neurosurgery, Children's Hospital of Nanjing Medical University, Nanjing, China | [2]Nanjing Key Laboratory of Pediatrics, Children's Hospital of Nanjing Medical University, Nanjing, China

Correspondence: Qing Yan (yq3880752@hotmail.com) | Wei Zhou (weizhou@njmu.edu.cn) | Gang Wang (wang509111@163.com)

Received: 17 January 2025 | **Revised:** 10 April 2025 | **Accepted:** 29 April 2025

Funding: This research was supported by grants from the National Natural Science Foundation of China (Grant number: 82402946), Medical Scientific Research Project of Jiangsu Provincial Health Commission (Grant number: H2023116) and Key projects of Nanjing Municipal Health Commission (ZKX23049).

Keywords: craniosynostosis | *IL11RA* gene | novel pathogenic variants

ABSTRACT

Background: Craniosynostosis (CS), a heterogeneous craniofacial disorder caused by premature fusion of cranial sutures, is sub-classified anatomically by suture involvement (sagittal, metopic, coronal, lambdoid) and phenotypically into isolated/non-syndromic forms or syndromic (CS with extracranial anomalies). Pathogenic variants in multiple genetic loci have been implicated in CS, with particular significance attributed to allelic variants in *IL11RA* (interleukin-11 receptor alpha subunit; OMIM#600939). Clinical observations of individuals with *IL11RA* mutations indicate syndromic CS, characterized by dental anomalies and Crouzon-like facial features.

Methods: Genetic analyses were carried out utilizing whole-exome sequencing, with subsequent validation through direct Sanger sequencing. *IL11RA* biallelic pathogenic variants were detected and further analyzed by multiple in silico prediction tools, including 3D protein modeling.

Results: Our cohort comprises six pediatric patients presenting with CS linked to biallelic pathogenic mutations in *IL11RA*, including two previously unreported variants (p.Pro218Argfs*140, p.Trp132Ter). Three-dimensional protein structure modeling and molecular docking simulations demonstrated that four missense variants (p.Pro116Leu, p.Glu126Gly, p.Gly231Val, p.Leu236Pro) disrupt hydrogen bond networks critical for maintaining the IL-11 receptor alpha subunit's tertiary structure, significantly reducing ligand-binding affinity to both interleukin-11 (IL-11) and gp130.

Conclusion: This study describes the clinical phenotype of six children with craniosynostosis and reveals novel variants in the *IL11RA* gene, thereby broadening the genotypic spectrum associated with this gene. Given the scarcity of patients reported in the literature, a detailed examination of the specific clinical and molecular characteristics will benefit our understanding of craniosynostosis caused by *IL11RA* variants.

1 | Introduction

Craniosynostosis (CS) is a condition characterized by the premature fusion of skull sutures that often occurs prenatally and is observed in about 1 out of 2500 newborns (Wilkie 2000). It presents a spectrum of clinical manifestations, including abnormalities in head shape, potential cognitive impairment, and other associated craniofacial features. Etiological investigations suggest that

Ziwei Liu and Ding Zhou contributed equally to this study.

craniosynostosis results from dysregulated suture closure. This process, which is intricately regulated by the activity of mesenchymal stem cells at the sutures, is disrupted due to imbalances in the proliferation and differentiation of osteoprogenitors, osteoblasts, and osteoclasts during membranous ossification (Zhao et al. 2015; Wilk et al. 2017; Guo et al. 2018; Bok et al. 2023). Advancements in human genetics over the past two decades have reshaped our comprehension of the molecular mechanisms driving craniosynostosis. To date, pathogenic variants in over 90 genes have been identified as causative factors for craniosynostosis, involving fibroblast growth factor, transforming growth factor beta, and Eph/ephrin signaling pathway-associated factors (Iseki et al. 1997; Rice et al. 2000; Twigg et al. 2004).

IL11RA gene encodes the interleukin-11 (IL-11) receptor (IL-11R), a type-I transmembrane protein that consists of an Ig-like domain (D1 domain), followed by two fibronectin type III domains (the D2 and D3 domains). IL-11 binds to the membrane-bound IL-11R, recruiting a homodimer of the signal-transducing β-receptor gp130. This interaction activates downstream signaling pathways that are crucial for osteoblast/osteoclast differentiation and the maintenance of cranial suture homeostasis (Fourcin et al. 1994; Nandurkar et al. 1996; Sims et al. 2005). Murine knockout models demonstrate that IL-11/IL11Rα deficiency causes cranial growth impairment and premature suture fusion (Nieminen et al. 2011; Sims et al. 2005). Since 2011, biallelic mutations in the *IL11RA* gene have been linked to autosomal recessive craniosynostosis. Documented cases are limited to 23 families, presenting with heterogeneous clinical presentation, including both syndromic and non-syndromic CS (Nieminen et al. 2011; Keupp et al. 2013; Brischoux-Boucher et al. 2018; Korakavi et al. 2019; Nishimura et al. 2020). This highlights the complex genotype–phenotype relationship with inter- and intrafamilial variability. Although the clinical phenotypes of affected individuals vary widely, multisuture craniosynostosis is the most prevalent feature, with approximately 90% of patients having varying degrees of craniosynostosis. Additionally, dental anomalies are regarded as a major characteristic of *IL11RA*-related disorders. Recent advances in molecular diagnostics further validate the critical role of *IL11RA* in syndromic CS; the outcome of targeted NGS screening in patients with syndromic forms of CS indicated that *IL11RA* is an emerging core gene for pansynostosis and Crouzon-like phenotype (Topa et al. 2022).

In this study, we present six children with syndromic or non-syndromic craniosynostosis, in whom novel CS-associated variants in the *IL11RA* gene were identified and characterized. Through genetic analysis and protein structure prediction, we have conducted preliminary explorations into the pathogenic foundation of these newly recognized variants, with the aim of deepening our understanding of craniosynostosis and its underlying genetic factors.

2 | Materials and Methods

2.1 | Participants

This study was approved by the Ethics Committee of Children's Hospital of Nanjing Medical University (202312004–1). We conducted a retrospectively cohort study involving 152 family trios with craniosynostosis (CS) who underwent trio-based whole exome sequencing (Trio-WES) between January 2018 and January 2024. Six families carrying *IL11RA* gene variants were subsequently identified in the cohort. Participants were referred to us by their pediatric neurosurgeons, with all patients undergoing standardized diagnostic evaluations including detailed physical examinations and multimodal neuroimaging (3D cranial CT reconstruction and brain MRI). The inclusion criteria including: (1) radiologically confirmed isolated or multisuture synostosis, and/or (2) presence of syndromic features (neurodevelopmental abnormalities, limb malformations, or characteristic dysmorphic facies) combined with either positive family history. The Chinese version of the Communication and Symbolic Behavior Scale-Developmental Profile (CSBS-DP) was used to assess children's language development in this study.

2.2 | Whole Exome Sequencing and Validation

Trio-WES was performed on probands and their parents using genomic DNA extracted from peripheral blood following the genome extraction kit instructions (Tiangen, China). Sequencing libraries were prepared following manufacturer protocols and paired-end sequenced (2×100 bp) on an Illumina HiSeq 2000 platform (Bio-Rad, Hercules, CA, USA). Raw data were processed to filter variants with $>1\%$ allele frequency in population databases (dbSNP, 1000 Genomes, ExAC, gnomAD, and an in-house Chinese cohort). Pathogenicity classification followed ACMG guidelines (Richards et al. 2015), with validation of candidate variants through bidirectional Sanger sequencing.

2.3 | Mutation Analysis of *IL11RA*

Variants were annotated against the IL11RA MANE Select transcript (NM_001142784.3) following HGVS nomenclature. Population allele frequencies were assessed using gnomAD v2.1.1 and ClinVar, while computational predictions employed PolyPhen-2 (v2.2.2), MutationTaster (2021), CADD (v1.6), and NMDEscPredictor. Evolutionary conservation was analyzed via Clustal Omega multiple sequence alignment (EMBL-EBI). Protein structural impacts were visualized using STRING-db (v12.0) and PyMOL v2.5, with molecular docking simulations performed through HDOCK server (Yan et al. 2020) using the IL-11Δ10/IL-11RαD1-D3/gp130D1-D3 complex (PDB ID 8DPT) as template. Mutant structures were generated via AlphaFold3 and interface interactions analyzed using PDBePISA.

2.4 | Literature Review

A systematic review of *IL11RA* variants was conducted through PubMed searches ("IL11RA" AND ["variant" OR "mutation"]) and HGMD Professional (v2023.4), covering publications through December 2023. All variants were indicated on the MANE Select transcript (NM_001142784.3) unless specified differently, according to Human Genome Variation Society (HGVS) guidelines (https://www.hgvs.org/mutnomen), with clinical annotations compiled in Table S1.

3 | Results

3.1 | Clinical Information

The six patients exhibited varying patterns of craniosynostosis, ranging from isolated coronal synostosis to complex multisuture involvement. Three patients (Patients 1, 3, 4) presented with pansynostosis, one (Patient 2) had sagittal and right lambdoid synostosis, one (Patients 5) had right coronal synostosis, and one (Patient 6) had metopic and bicoronal synostosis. The age at diagnosis varied from the neonatal period (Patient 6) to 3.3 years (Patient 1). Only Patient 2 had isolated craniosynostosis without other extracranial symptoms. On MRI, both Patient 1 and Patient 4 showed Chiari I malformation. Patient 3 and Patient 6 shared a Crouzon-like phenotype, characterized by midface hypoplasia and exophthalmos. For Patient 6, given his young age, an assessment of tooth development was not warranted. Detailed synostosis patterns and associated phenotypes are summarized in Table 1. All patients in this study received neuroendoscopic craniofacial reconstruction surgery at our hospital, resulting in significant improvement in their head shapes. Comprehensive imaging datasets, including clinical photographs, three-dimensional cranial CT reconstructions, and brain MRI, are presented in Figure 1.

3.2 | Results of the Genetic Screening

Whole-exome sequencing (WES) of six probands and their parents revealed eight distinct *IL11RA* variants, including four missense variants (p. Pro116Leu, p. Glu126Gly, p. Gly231Val and p. Leu236Pro), two nonsense variants (p. Trp132Ter and p. Arg234Ter), one frameshift variant (p. Pro218Argfs*140) and one splice-site variant (c.811-2A>G). As illustrated in Figure 2A, all identified exonic variants clustered within the extracellular D2 and D3 domains of IL-11RA, which mediate ligand-receptor binding by orchestrating the structural interface between IL-11Rα and the IL-11/gp130 signaling complex.

Notably, all identified *IL11RA* variants in this cohort constitute novel genotype–phenotype associations with CS, with the exception of p.Leu236Pro, which has been previously reported by Nishimura et al. (2020). The remaining seven variants, with the exception of p.Pro218Argfs*140 and p.Trp132Ter, were

TABLE 1 | Phenotypic characteristics of six pediatric patients with CS.

Patient	1	2	3	4	5	6
Age at diagnoses (y)	3.3 year	1 year	11 months	1.8 year	3 months	1 months
OFC(cm)	49.4 (50th)	46.2 (50th)	44.4 (15th)	45 (< 5th)	40 (50th)	33 (< 3th)
CRS	P	S, RL	P	P	RC	M, BC
Crouzon-like phenotype	No	No	Yes	No	No	Yes
Forehead	Normal	Normal	Protruding	Normal	Asymmetric	Flat
Midface hypoplasia	No	No	Yes	No	Yes	Yes
Exophthalmos	No	No	Yes	No	No	Yes
Delayed tooth eruption	No	No	Yes	No	No	—
Dental malalignment	No	No	No	Yes	No	No
Malocclusion	No	No	Yes	Yes	No	—
Supernumerary teeth	No	No	Yes	No	No	—
Skull shape	Scaphocephaly	Scaphocephaly	Trigonocephaly	Scaphocephaly	Anterior plagiocephaly	Microcephaly brachycephaly
Language development delay	Yes	No	Yes	No	No	No
Chiari I	Yes	No	No	Yes	No	No
Other	—	—	—	—	Atrial septal defect	—

Abbreviations: BC, bicoronall; CRS, sutures fused in craniosynostosis; M, metopic; P, pansynostosis; RC, right coronal; RL, right lambdoid; S, sagittal.

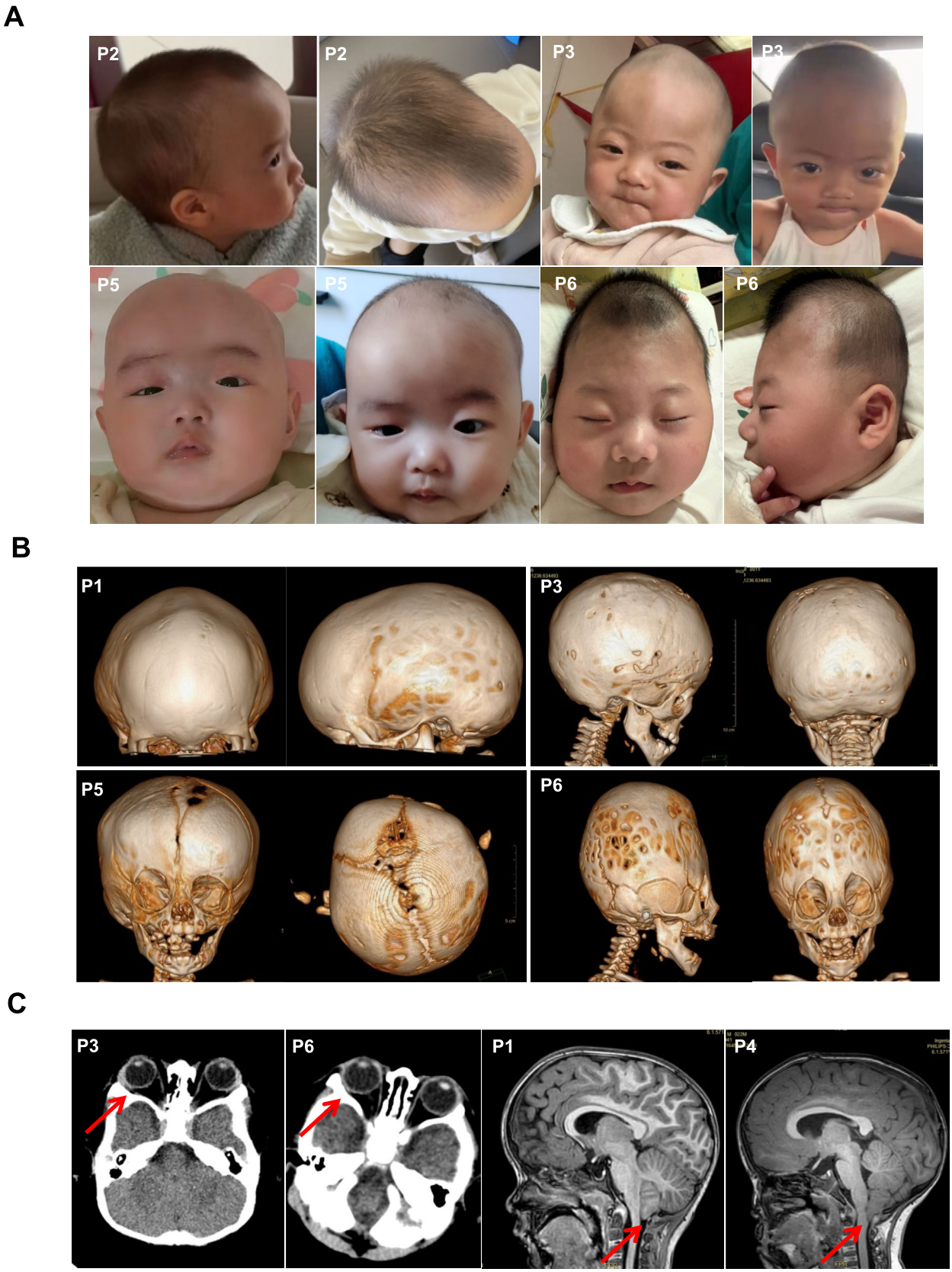

FIGURE 1 | Photographs, three-dimensional CT scans of skull and magnetic resonance imaging (MRI) of patients. (A) Facial photographs of Patients 2,3,5 and 6. Patient 3 and 6 demonstrating characteristic Crouzon-like craniofacial features including frontal bossing, midface hypoplasia, and orbital proptosis. (B) Three-dimensional reconstructed cranial CT scans of patient 1,3,5, and 6. Patient 1,3 and 6 showed pansynostosis. Patient 5 isolated closure of the right coronal suture. (C) Representative brain MRI findings (axial T2-weighted and sagittal T1-weighted images) in Patient 1,3,4 and 6. Patient 1 and 6 showing exophthalmos (red arrow). Patient 1 and 4 showing Chiari I malformation (red arrow).

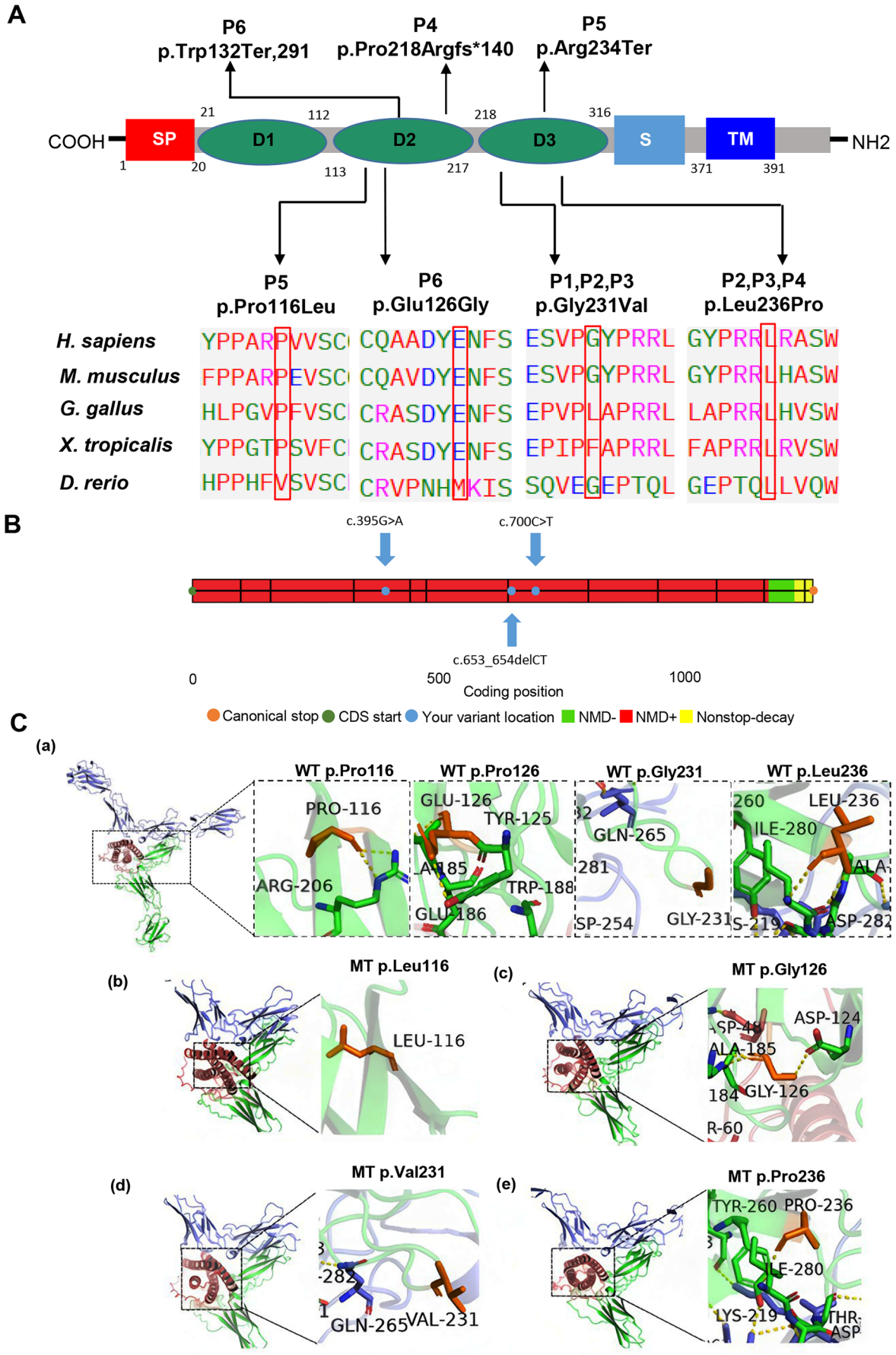

FIGURE 2 | Legend on next page.

FIGURE 2 | (A)Depicts the protein structure of human IL11RA showing the positions of the variants. Evolutionary conservation of amino acid position Pro116, Glu126, Gly231 and Leu236 in IL11RA protein across evolution. D1–D3, immunoglobulin-like domains 1–3; S, stalk region; SP, signal peptide; TM, transmembrane region. (B) Schematic representation of the *IL11RA* gene showing the localization of truncating variants (p. Trp132Ter and p. Arg234Ter) and frameshift variant (p. Pro218Argfs*140) all subjecting (NMD+) to nonsense mediated RNA decay (https://nmdpredictions.shinyapps.io/shiny/). The region of *IL11RA* where truncating variants trigger NMD is indicated in green. (C) Structural modeling of wild-type (WT) versus mutant (MUT) IL11RA. Comparative analysis reveals disrupted hydrogen bonding networks (dashed lines) between mutant residues (Pro116Leu, Glu126Gly, Gly231Val, Leu236Pro) and adjacent amino acids, suggesting destabilization of domain tertiary structure.

present at extremely low frequencies (minor allele frequency, MAF <0.05) in population databases, including gnomAD, dbSNP, and ClinVar. p.Gly231Val has been reported in ClinVar at the same amino acid position but with different amino acid substitutions. Truncating variants (p.Trp132Ter, p.Arg234Ter and p. Pro218Argfs*140) were predicted to be subject to degradation by nonsense-mediated decay (Figure 2B). c.811-2A>G in intron 8 was a classical splice site variant and was computationally validated to abrogate normal splicing of exon 9. Analysis using MaxEntScan demonstrated a severe loss of splice site strength, with the score dropping from 9.46 (wild-type) to 1.51 (mutant). In accordance with ACMG guidelines, all variants were classified as pathogenic or likely pathogenic, except p. Pro116Leu and p. Glu126Gly. These two variants were categorized as variants of uncertain significance (VUS) due to insufficient functional validation. Specific variant information is listed in Table 2.

3.3 | Protein Structure Modeling

To evaluate the pathogenicity of these *IL11RA* variants, we constructed 3D structural models of the wild-type and mutant using AlphaFold3 (Figure 2C). Structural comparisons revealed significant disruption in hydrogen bonding formation and steric clashes at the mutation sites. In the wild-type (WT) IL-11Ra structure, Pro116 forms two hydrogen bonds with Arg206, stabilizing the local conformation. Substitution of Pro116 with the bulkier Leu116 residue disrupts both bonds, introducing steric clashes that destabilize the D2 domain. Similarly, Glu126 in the WT IL-11Ra engages in two hydrogen bonds with Tyr125 and Ala185. Mutation to Gly126 (a structurally flexible residue) eliminates these bonds while forming three new hydrogen bonds with Asp124 and Ala185, altering the electrostatic landscape and potentially perturbing receptor dimerization. In contrast, substitution of Leu236 (a hydrophobic residue) with Pro236 (a rigid cyclic amino acid) reduces hydrogen bonding from two to one, compromising interdomain packing. Notably, the p. Gly231Val variant preserves hydrogen bonding networks but introduces a valine side chain that may alter helical geometry. Collectively, these structural perturbations—reduced hydrogen bonding, increased steric strain, and altered domain interfaces—likely impair IL-11Ra folding, ligand binding, or signaling competency.

To assess the impact of *IL11RA* variants on ligand binding affinity within the IL-11/IL-11R/gp130 signaling complex, we performed computational docking simulations using the wild-type (WT) and mutant C-terminal truncated IL-11Rα (IL-11RαΔD1-D3) structures. The WT IL-11RαΔD1-D3 exhibited a strong binding free energy of −19.68 kcal/mol with IL-11 and gp130. In contrast, all four mutants (p.Pro116Leu, p.Glu126Gly, p.Gly231Val, p.Leu236Pro) displayed increased binding free energy compared to WT, indicating reduced binding affinity for the IL-11R-gp130-IL11 complex (Table 3). Structural analysis of hydrogen bonding interactions between IL-11R and the IL-11/gp130 complex revealed that the p.Pro116Leu mutation disrupted hydrogen bonds between IL-11R and both IL-11 and gp130. In contrast, the p.Glu126Gly, p.Gly231Val, and p.Leu-236Pro mutations exhibited enhanced hydrogen bonding with IL-11 but reduced interactions with gp130 (Table S2). These findings indicate that these missense variants potentially disrupt IL-11R-gp130-IL-11 ternary complex formation.

4 | Discussion

In this study, we expand the genotypic and phenotypic spectrum of IL11RA-associated craniosynostosis by reporting six unrelated pediatric patients with compound heterozygous variants. The synostosis pattern associated with *IL11RA* mutations exhibits an insidious progression, which differs from other syndromic forms. While multisuture involvement emerged as a hallmark (observed in 89% of reported patients), five patients in our cohort developed pansynostosis or multisuture craniosynostosis. Following the development of multisuture craniosynostosis, midface hypoplasia emerged as the most prevalent associated feature, observed in 50% of our cohort. Compared to prior reports, the patients in our cohort exhibited younger diagnostic ages, with a median age of 11.5 months. Patient 1, the eldest in our cohort, presented with pansynostosis at diagnosis but without significant midface/maxillary hypoplasia. For Patient 6, with neonatal-onset sutural closure, midface hypoplasia and exophthalmos face a high risk of progressive pansynostosis and dental anomalies. Significantly, midface hypoplasia demonstrates significant phenotypic plasticity; while it primarily manifests as hypoplasia of the orbital floor and zygomatic arches in infancy, its progression leads to secondary ocular proptosis, mandibular prognathism, and malocclusion during childhood development. These findings highlight the need for longitudinal 3D-CT surveillance to detect occult disease progression, as clinical evaluation alone may underestimate synostosis severity.

Comparative analysis of our cohort with 23 previously reported familial cases (Table S1) revealed distinct genetic architectures; 75% of literature-documented patients exhibited homozygous pathogenic variants, while all six patients in our cohort harbored compound heterozygous variants (Figures S1 and S2). Notably, two patients in our cohort (Patient 2 and Patient 3) harbored identical compound heterozygous variants (p.Leu236Pro and p.Gly231Val) yet exhibited markedly discordant clinical severity. Patient 2 presented with non-syndromic multisuture synostosis, whereas Patient 3 demonstrated syndromic features

TABLE 2 | Variants of the *IL11RA* gene identified in this study.

No.	GRCh37/ hg19 Pos	Nucleotide change	Amino acid change	Exon/ Intron	GnomAD (hom/het/ allele count)	dbSNP/Clinvar ID	Mutation taster	CADD	ACMG classification
1	chr9:34658562	c.692G>T	p.Gly231Val	8	0/38/282716	rs74968235/NA	Disease causing	Deleterious	Likely pathogenic
2	chr9:34659754	c.811-2A>G	p.?	IVS8	0/3/251358	rs200169943/2022980	Disease causing	Deleterious	Pathogenic
3	chr9:34658577	c.707T>C	p.Leu236Pro	8	0/1/251326	rs769726217/NA	Disease causing	Deleterious	Likely pathogenic
4	chr9:34658523–34,658,524	c.653_654delCT	p.Pro218Argfs*140	8	NA	NA/NA	/	/	Likely pathogenic
5	chr9:34658570	c.700C>T	p.Arg234Ter	8	0/8/282722	rs778089627/NA	Disease causing	Deleterious	Likely pathogenic
6	chr9:34657047	c.347C>T	p.Pro116Leu	5	0/1/31378	rs1465759522/546145	Disease causing	Deleterious	Uncertain significance
7	chr9:34657095	c.395G>A	p.Trp132Ter	5	NA	NA/NA	Disease causing	Deleterious	Likely pathogenic
8	chr9:34657077	c.377A>G	p.Glu126Gly	5	0/6/251492	rs755185119/NA	Disease causing	Deleterious	Uncertain significance

TABLE 3 | Changes in the interaction between wild-type and mutant IL11RA and IL-11/gp130 protein complexes.

	Protein docking score with protein IL-11/gp130	Binding free energy (kcal/mol)	Docking area (Å)
$IL11RA^{wt}$	−450.82	−19.68	1726
$IL11RA^{Leu116}$	−283.17	−12.36	1868
$IL11RA^{Gly126}$	−278.22	−12.15	1860
$IL11RA^{Val231}$	−307.34	−13.42	1872
$IL11RA^{Pro236}$	−301.72	−13.17	1925

including specific features, e.g., midface hypoplasia, dental anomalies, and language development delay. The p.Leu236Pro variant, originally reported in a homozygous state caused by maternal uniparental isodisomy (UPD) of chromosome 9 in a Japanese patient with multisuture synostosis and characteristic craniofacial dysmorphism (Nishimura et al. 2020), illustrates this dual-layered genetic heterogeneity, encompassing both interfamilial diversity and intrafamilial phenotypic variability, which has been previously documented among affected members within single pedigrees in (Brischoux-Boucher et al. 2018), reinforcing the complex genotype–phenotype characteristics of *IL11RA*-related disorders. Our findings further underscore the heightened genetic complexity of *IL11RA*-associated CS within East Asian populations, potentially influenced by population-specific modifier genes or epigenetic regulatory mechanisms.

Despite extensive reporting of *IL11RA* mutations, the molecular mechanisms underlying IL-11 receptor dysfunction in craniosynostosis remain poorly elucidated. Current evidence suggests that pathogenic variants primarily disrupt IL-11R maturation and membrane trafficking, leading to impaired IL-11 signaling during craniofacial development (Agthe et al. 2018; Ahmad et al. 2023; Sims and Griffin 2024; Kespohl et al. 2024). Notably, all previously reported CS-associated variants localized to the extracellular D1-D3 ligand-binding domains, except for p.Glu364_Val368del in the stalk region (Kespohl et al. 2024). Structural analyses have elucidated the mechanistic significance of the tryptophan-arginine zipper topology within the D3 domain, demonstrating its dual functionality in orchestrating receptor tertiary structure stabilization and cytokine signaling competency. Pathogenic variants disrupting this architectural motif (e.g., p.R296W) exhibit pleiotropic effects, including endoplasmic reticulum (ER) retention and impairment of downstream signaling cascades (Agthe et al. 2018; Olsen and Kragelund 2014; Nieminen et al. 2011; Sentosa et al. 2024). In our cohort, novel CS-associated variants are primarily located within the D2 and D3 domains, sparing the Trp-Arg zipper motif while preserving its hydrogen bonding network. Structural modeling revealed that compared to wild type IL-11Ra, mutants p.Glu126Gly, p.Gly231Val, and p.Leu236Pro exhibited enhanced IL-11 binding but reduced gp130 engagement, destabilizing the ternary IL-11/IL-11R/gp130 complex. Notably, prior reports indicate homozygous truncating mutations confer more severe phenotypes compared to missense variants, likely due to complete loss of receptor function (Nieminen et al. 2011; Keupp et al. 2013; Brischoux-Boucher et al. 2018; Topa et al. 2022; Ahmad et al. 2023). The truncating mutation disrupts IL-11R maturation and membrane trafficking, while the missense variant further destabilizes ligand-receptor interactions, as demonstrated by structural modeling. This synergistic disruption could abolish IL-11 signaling during critical periods of cranial suture development, explaining the neonatal-onset multisuture craniosynostosis and severe midface hypoplasia observed in Patient 6.

Collectively, we report six pediatric patients with craniosynostosis and identify seven novel IL11RA variants associated with craniosynostosis (CS). Through rigorous in silico analyses, we provide robust computational evidence supporting the pathogenicity of novel missense variants, elucidating their disruptive effects on protein stability and ligand-binding affinity. While recognizing the constraints of a limited sample size and incomplete functional validation, we propose an integrated diagnostic framework that synergizes computational variant impact analysis with comprehensive clinical phenotyping to improve diagnostic accuracy and specificity. Future functional investigations such as cell-based assays and animal models are essential to elucidate the mechanistic basis of IL-11R dysfunction and establish robust genotype–phenotype correlations in genetically heterogeneous populations. Our findings also reinforce the necessity of molecular screening in early-onset craniosynostosis cases through targeted gene panel analysis incorporating *IL11RA*. Longitudinal follow-up and multidisciplinary care are imperative to optimize outcomes for individuals with *IL11RA* variants. Ultimately, this work not only expands the genetic architecture of CS but also establishes a paradigm for precision medicine approaches in rare skeletal disorders, emphasizing the synergistic integration of computational biology, molecular diagnostics, and clinical care.

Author Contributions

Ziwei Liu, Wei Zhou gathered clinical information of the patients and drafted the manuscript. Qing Yan, Gang Wang diagnosed the patients and designed this study. Ding Zhou, Chunli Wang, and Bixia Zheng contributed to the checking of the revision, genetic evaluation, and gene databases analysis. All authors reviewed, read, and approved the final manuscript.

Acknowledgments

We would like to thank the families and study individuals for their contribution. We also thank the Chigene (Beijing, China), Translational Medical Research Center Co. Ltd., for whole exome sequencing.

Ethics Statement

The study was approved by the ethical committee of the Ethics Committee of Children's Hospital of Nanjing Medical University (202312004-1) and informed consent was obtained from legal guardians, with all identifiers removed to protect patient confidentiality.

Conflicts of Interest

The authors declare no conflicts of interest.

Data Availability Statement

The data that support the findings of this study are available on request from the corresponding author. The data are not publicly available due to privacy or ethical restrictions.

References

Agthe, M., J. Brügge, Y. Garbers, et al. 2018. "Mutations in Craniosynostosis Patients Cause Defective Interleukin-11 Receptor Maturation and Drive Craniosynostosis-Like Disease in Mice." *Cell Reports* 25, no. 1: 10–18. https://doi.org/10.1016/j.celrep.2018.09.005.

Ahmad, I., J. Lokau, B. Kespohl, et al. 2023. "The Interleukin-11 Receptor Variant p.W307R Results in Craniosynostosis in Humans." *Scientific Reports* 13, no. 1: 13479. https://doi.org/10.1038/s41598-023-39466-y.

Bok, S., A. R. Yallowitz, J. Sun, et al. 2023. "A Multi-Stem Cell Basis for Craniosynostosis and Calvarial Mineralization." *Nature* 621, no. 7980: 804–812. https://doi.org/10.1038/s41586-023-06526-2.

Brischoux-Boucher, E., A. Trimouille, G. Baujat, et al. 2018. "IL11RA-Related Crouzon-Like Autosomal Recessive Craniosynostosis in 10 New Patients: Resemblances and Differences." *Clinical Genetics* 94, no. 3: 373–380. https://doi.org/10.1111/cge.13409.

Fourcin, M., S. Chevalier, J. J. Lebrun, et al. 1994. "Involvement of gp130/Interleukin-6 Receptor Transducing Component in Interleukin-11 Receptor." *European Journal of Immunology* 24, no. 1: 277–280. https://doi.org/10.1002/eji.1830240143.

Guo, Y., Y. Yuan, L. Wu, et al. 2018. "BMP-IHH-Mediated Interplay Between Mesenchymal Stem Cells and Osteoclasts Supports Calvarial Bone Homeostasis and Repair." *Bone Research* 6: 30. https://doi.org/10.1038/s41413-018-0031-x.

Iseki, S., A. O. Wilkie, J. K. Heath, T. Ishimaru, K. Eto, and G. M. Morriss-Kay. 1997. "Fgfr2 and Osteopontin Domains in the Developing Skull Vault Are Mutually Exclusive and Can Be Altered by Locally Applied FGF2." *Development (Cambridge, England)* 124, no. 17: 3375–3384. https://doi.org/10.1242/dev.124.17.3375.

Kespohl, B., A. L. Hegele, S. Düsterhöft, et al. 2024. "Molecular Characterization of the Craniosynostosis-Associated Interleukin-11 Receptor Variants p.T306_S308dup and p.E364_V368del." *FEBS Journal* 291, no. 8: 1667–1683. https://doi.org/10.1111/febs.17015.

Keupp, K., Y. Li, I. Vargel, et al. 2013. "Mutations in the Interleukin Receptor IL11RA Cause Autosomal Recessive Crouzon-Like Craniosynostosis." *Molecular Genetics & Genomic Medicine* 1, no. 4: 223–237. https://doi.org/10.1002/mgg3.28.

Korakavi, N., J. W. Prokop, and L. H. Seaver. 2019. "Evolution of the Phenotype of Craniosynostosis With Dental Anomalies Syndrome and Report of IL11RA Variant Population Frequencies in a Crouzon-Like Autosomal Recessive Syndrome." *American Journal of Medical Genetics. Part A* 179, no. 4: 668–673. https://doi.org/10.1002/ajmg.a.61070.

Nandurkar, H. H., D. J. Hilton, P. Nathan, T. Willson, N. Nicola, and C. G. Begley. 1996. "The Human IL-11 Receptor Requires gp130 for Signalling: Demonstration by Molecular Cloning of the Receptor." *Oncogene* 12, no. 3: 585–593.

Nieminen, P., N. V. Morgan, A. L. Fenwick, et al. 2011. "Inactivation of IL11 Signaling Causes Craniosynostosis, Delayed Tooth Eruption, and Supernumerary Teeth." *American Journal of Human Genetics* 89, no. 1: 67–81. https://doi.org/10.1016/j.ajhg.2011.05.024.

Nishimura, N., H. Murakami, T. Hayashi, H. Sato, and K. Kurosawa. 2020. "Multiple Craniosynostosis and Facial Dysmorphisms With Homozygous IL11RA Variant Caused by Maternal Uniparental Isodisomy of Chromosome 9." *Congenital Anomalies* 60, no. 5: 153–155. https://doi.org/10.1111/cga.12371.

Olsen, J. G., and B. B. Kragelund. 2014. "Who Climbs the Tryptophan Ladder? On the Structure and Function of the WSXWS Motif in Cytokine Receptors and Thrombospondin Repeats." *Cytokine & Growth Factor Reviews* 25, no. 3: 337–341. https://doi.org/10.1016/j.cytogfr.2014.04.007.

Rice, D. P., T. Aberg, Y. Chan, et al. 2000. "Integration of FGF and TWIST in Calvarial Bone and Suture Development." *Development (Cambridge, England)* 127, no. 9: 1845–1855. https://doi.org/10.1242/dev.127.9.1845.

Richards, S., N. Aziz, S. Bale, et al. 2015. "Standards and Guidelines for the Interpretation of Sequence Variants: A Joint Consensus Recommendation of the American College of Medical Genetics and Genomics and the Association for Molecular Pathology." *Genetics in Medicine: Official Journal of the American College of Medical Genetics* 17, no. 5: 405–424. https://doi.org/10.1038/gim.2015.30.

Sentosa, D. D., R. D. Metcalfe, N. A. Sims, T. L. Putoczki, and M. D. W. Griffin. 2024. "The Structure of the IL-11 Signalling Complex Provides Insight Into Receptor Variants Associated With Craniosynostosis." *FEBS Journal* 292, no. 3: 500–509. https://doi.org/10.1111/febs.17307.

Sims, N. A., and M. D. W. Griffin. 2024. "Craniosynostosis-Associated Variants in the IL-11R Complex: New Insights and Questions." *FEBS Journal* 291, no. 8: 1663–1666. https://doi.org/10.1111/febs.17078.

Sims, N. A., B. J. Jenkins, A. Nakamura, et al. 2005. "Interleukin-11 Receptor Signaling Is Required for Normal Bone Remodeling." *Journal of Bone and Mineral Research: the Official Journal of the American Society for Bone and Mineral Research* 20, no. 7: 1093–1102. https://doi.org/10.1359/JBMR.050209.

Topa, A., A. Rohlin, M. K. Andersson, et al. 2022. "The Outcome of Targeted NGS Screening in Patients With Syndromic Forms of Sagittal and Pansynostosis—IL11RA Is an Emerging Core-Gene for Pansynostosis." *European Journal of Medical Genetics* 65, no. 5: 104476. https://doi.org/10.1016/j.ejmg.2022.104476.

Twigg, S. R., R. Kan, C. Babbs, et al. 2004. "Mutations of Ephrin-B1 (EFNB1), a Marker of Tissue Boundary Formation, Cause Craniofrontonasal Syndrome." *Proceedings of the National Academy of Sciences of the United States of America* 101, no. 23: 8652–8657. https://doi.org/10.1073/pnas.0402819101.

Wilk, K., S. A. Yeh, L. J. Mortensen, et al. 2017. "Postnatal Calvarial Skeletal Stem Cells Expressing PRX1 Reside Exclusively in the Calvarial Sutures and Are Required for Bone Regeneration." *Stem Cell Reports* 8, no. 4: 933–946. https://doi.org/10.1016/j.stemcr.2017.03.002.

Wilkie, A. O. 2000. "Epidemiology and Genetics of Craniosynostosis." *American Journal of Medical Genetics* 90, no. 1: 82–84.

Yan, Y., H. Tao, J. He, and S. Y. Huang. 2020. "The HDOCK Server for Integrated Protein-Protein Docking." *Nature Protocols* 15, no. 5: 1829–1852. https://doi.org/10.1038/s41596-020-0312-x.

Zhao, H., J. Feng, T. V. Ho, W. Grimes, M. Urata, and Y. Chai. 2015. "The Suture Provides a Niche for Mesenchymal Stem Cells of Craniofacial Bones." *Nature Cell Biology* 17, no. 4: 386–396. https://doi.org/10.1038/ncb3139.

Supporting Information

Additional supporting information can be found online in the Supporting Information section.